Chinese Journal of
POLYMER SCIENCE

REVIEW

https://doi.org/10.1007/s10118-020-2380-3
Chinese J. Polym. Sci. **2020**, *38*, 565–578

Physical Properties of Polymers under Soft and Hard Nanoconfinement: A Review

Ming-Chao Ma[a] and Yun-Long Guo[a,b*]

[a] *University of Michigan-Shanghai Jiao Tong University Joint Institute, Shanghai Jiao Tong University, Shanghai 200240, China*
[b] *School of Materials Science and Engineering, Shanghai Jiao Tong University, Shanghai 200240, China*

Abstract Polymeric materials under nanoconfinements have substantially deviated physical properties with respect to the bulk, especially glass transition temperature, physical aging, and crystallization behavior. Here we highlight the leading methods for creating various confinement systems. Upon these systems, recent advances on hard and soft confinement effect for glass transition, physical aging, mechanical properties and crystallization of polymers are reviewed in details. Furthermore, as nanoconfined systems in extreme conditions are experimentally inaccessible, simulation results describing confinement effect on such systems are also discussed.

Keywords Nanoconfinement; Glass transition temperature; Physical aging; Mechanical properties; Crystallization

Citation: Ma, M. C.; Guo, Y. L. Physical properties of polymers under soft and hard nanoconfinement: a review. *Chinese J. Polym. Sci.* **2020**, *38*, 565–578.

INTRODUCTION

The states of polymeric materials are temperature dependent as shown in Fig. 1. The enthalpy, volume or other properties have different temperature dependence in two distinct states, *i.e.*, glass state and liquid state. The intersection of the glass and liquid state lines corresponds to one crucial temperature for state transition which is referred to as glass transition temperature (T_g). Polymeric materials are in equilibrium state above T_g. In contrast, the physical properties, including but not limited to volume,[1–3] enthalpy,[4–6] gas permeability[7–9] and elastic modulus,[10–12] gradually change with time if the polymers are annealed below T_g. This evolution process is physical aging or structure relaxation. These time-dependent thermodynamic properties are attributed to macromolecular motion whose mode and intensity are relevant to the molecular mobility.

Polymeric materials under confinement originated from size effect, interfacial effect and spatial constraints have substantially different thermodynamic or mechanical properties from the bulk, as mobility of polymer chains is altered by confinement effect. For instance, the T_g of polymers on silica substrate can be enhanced or decreased up to more than 30 °C from the bulk value.[13] And in particular, the aging rate of PS blocks in a PS-*b*-PMMA copolymer can be accelerated by a factor of three compared to that of neat PS with similar molecular weight.[14] Confinement can be classified into hard confinement and soft confinement, according to the relative modulus between polymer and interfacial materials.

In addition to the physical aging of amorphous materials, crystallization of polymers is greatly influenced by confinement. Together with mechanical properties, almost all concerned aspects of polymers are influenced by the effect of confinement. In the last several decades, the deviated physical properties under soft and hard confinement have attracted remarkable interests. A great deal of efforts have been taken to explore and rationalize the mechanism of the nanoscale confinement effect. Despite some advances, the underlying physics of confinement effect of polymers has not been well understood.

In this review, we highlight the methods for creating the model systems to investigate confinement effect under different geometries and dimensions, and summarize the major progress of the hard and soft confinement effect, on T_g, structural relaxation, mechanical properties, and crystallization of polymers in recent works. Moreover, the applications of confined systems are emphasized, especially for which the better manipulation of properties of confined polymers will benefit the future design and applications. Although this work mainly focuses on the experimental results, the models or simulation methods for describing the confinement effect are also discussed.

METHODS FOR CREATING CONFINEMENT

The confinement systems can be created by various means, either from fundamental methods or using novel techniques. A major method of confinement creation is making thin films by spin coating or solution casting, as they have a very simple preparation process and create adjustable confinement provided by interface when the thickness is less than some thres-

* Corresponding author, E-mail: yunlong.guo@sjtu.edu.cn
Received September 15, 2019; Accepted December 2, 2019; Published online February 18, 2020

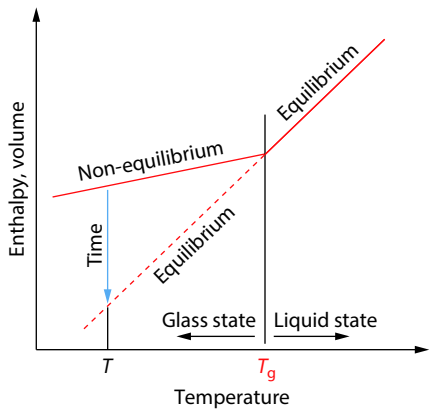

Fig. 1 Typical temperature dependence of enthalpy and volume of a glass-forming polymer.

hold.[13,15–50] In general, hard substrates, including silica, quartz, mica, gold, aluminate, and polymers with relatively high Young's modulus, are used to provide the hard confinement.[13,15–33] On the other hand, soft confinement conditions are achieved by the free-standing surface, liquid interface, or the relatively soft polymer substrate.[13,15,16,19,24,27,29,31,32,36–50] Moreover, Murphy, Langhe and their coworkers reported that the complex alternating multilayer structure from stacked thin films can be produced by a layer-multiplying co-extrusion process, providing an efficient method for integrating multiple confinement from different interfaces.[51–53] The details of such co-extrusion process were introduced elsewhere.[54] Instead of the simple smooth interface, Yavari and coworkers used porous polyethersulfone to support thin films and thus providing special confinement effect.[34,35] Their work created a novel method for changing the 1D confinement condition for thin films and has great relevance in industrial application.

In addition to the 1D confinement in thin films, the hard or soft confinement can be achieved in 2D condition. Two main methods for creating 2D hard confinement have been introduced in recent works.[22,55–58] One of those is mixing the polymer solution with oriented carbon nanotubes to produce nanocomposites.[56] Instead of the nanotubes in nanocomposites, another 2D hard confinement environment was attained by placing polymers into nanoporous matrix like anodic aluminum oxide (AAO) template.[22,55,57,58] The nanoporous AAO template was filled with polymers, which is achieved by melting the polymer films on the top of AAO template to infiltrate at a suitable temperature. As such, the AAO matrix is able to provide 2D hard confinement to the polymer in the nano pores. On the other hand, a representative 2D soft confinement, *i.e.*, freely standing polymer nanowires, was created by electrospinning. This notable method is extruding the polymer solution from plastic syringe with a stainless steel needle to a substrate under high voltage.[58] Subsequently, the electrospun nanowires are dispersed in solution. By this method, the polymer nanowires with free surface can be attained for the purpose of studying the soft 2D confinement effect.

Polymer nanoparticles can provide the 3D free-standing surface (soft confinement)[59–63] and hard confinement after capping a rigid shell,[59,63,64] making them useful to investigate 3D confinement effect. Polymer nanoparticles can be synthesized by emulsion polymerization with the details reported elsewhere.[65] The limitation of this polymerization method is that it is difficult to control molecular weight and particle size independently. Given this fact, another method called flash nanoprecipitation was developed and used to overcome this difficulty when the particle diameter is no more than 150 nm. The details of this method were reported in the literature.[66] Upon polymer nanoparticles, a notable 3D hard confinement model is the core-shell model. For instance, Guo and coworkers synthesized the silica-capped PS nanoparticles by the Stöber method.[59,63,64] The dispersed PS nanospheres were reacted with ammonia and tetraethoxysilane to coat a thin layer of silica, after pretreating with polyelectrolytes in water, and the details were reported in literature.[66,67] Silica-capped PS nanoparticles provide not only the hard confinement, but also an isochoric condition for the PS particles inside. Instead of hard shell, Zhu and coworkers used gold as hard core in the core-shell structure.[68] The thiolated PS with $HAuCl_4{\cdot}3H_2O$ dissolved in distilled tetrahydrofuran (THF) reacted with $NaBH_4$ in THF-water solution to produce polystyrene-capped Au nanoparticles. The resulting material showed good core-shell structure and had substantially different properties from the bulk PS. In addition to nanoparticles, another typical method for creating 3D hard confinement is preparing nanocomposites by mixing the polymer with some hard nanoparticles typically made by silica or metallic oxides.[30,33,69–79] Sometimes, the surface of nanoparticles was functionalized to get better dispersibility.[69–76] On 3D confined materials, diblock copolymers were recently found to be an ideal model to study the 3D confinement effect,[14,80,81] as they can form various morphologies from self-assembled microphase separation, by controlling the molecular weight and molar ratio of the two components. These geometries formed by two polymer components with relatively soft and hard states provide the soft and hard confinements to each other simultaneously. This unprecedented method serves as a simpler and more efficient way to create 3D confinement with polymer-polymer interfaces.

With the confined polymers under various geometries and dimensions, the study of the hard and soft confinement effect on different properties becomes accessible. We review recent progress from such work in the following sections.

HARD CONFINEMENT EFFECT

Effect on T_g

The hard confinement effect on T_g does not hold complete consistency throughout the related research activities in the last several decades. Some results showed that T_gs of polymeric materials under hard confinement have substantial deviation from the T_gs of bulk materials. The deviation direction depends on the segmental mobility, restricted mobility for T_g enhancement[13,16,17,24–27,30,33,56,58,68,76–79,82,83] and enhanced mobility for T_g depression.[13,17,18,21,25,33,55,79,83–85] However, Sun and coworkers reported reduced mobility of PS films due to adsorbed layer, resulting in suppressed T_g, as opposed to the general correlation between mobility and deviation of T_g.[86] In contrast to altered T_g, other results showed invariant T_gs of polymers under hard confinement, with respect to the bulk

https://doi.org/10.1007/s10118-020-2380-3

value.[30,51,55,56,59,63,69,76,79] Fortunately, the T_g deviation showed consistent trend under large confinement intensity, regardless of the materials and confinement creation methods in many works.[16–18,21,25,30,33,68,73,75,77,87]

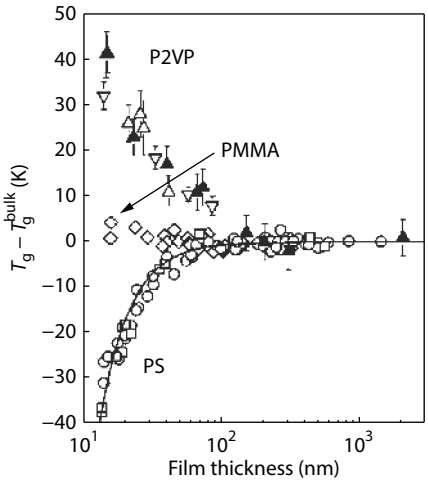

Fig. 2 T_g deviation of PS films (circles), PMMA films (diamonds) and P2VP films (triangles) on silica substrate with different film thicknesses. (Reprinted with permission from Ref. [13]; Copyright (2007) American Chemical Society).

Researchers dedicated to probing the underlying mechanism of hard confinement effect and a universal elucidation for these inconsistent of hard confinement effect on T_g. In general, the existence of T_g deviation depends on confinement intensity,[27,30,76] *i.e.*, the confinement-interface-to-internal-polymer ratio. For example, Koerner and coworkers found that the T_g of PS composited with SiO_2 remains the bulk value until the volume fraction of SiO_2 is greater than 40%.[76] Fakhraai and coworker indicated that the cooling rate dependence of T_g reduction is much stronger than the thickness dependence of T_g suppression, which gives an explanation to contradictory of hard confinement effect on T_g with different cooling rates.[88] In addition, molecular weight is a crucial factor of the existence of T_g deviation of polymers in the 2D hard nanoporous template.[55] When molecular weight of PS is larger than 175 kg/mol, the PS nanorods confined in AAO nanoporous template displays a lower T_g than the bulk, as the radius of gyration derived by molecular weight plays an important role in the intrinsic size effect.[55] The intrinsic size effect suppresses T_g when the chains packing are disturbed by the hard confinement. Moreover, adsorbed layer at interface is considered momentous in changing chains packing and mobility.[22,89,90] Several works interpreted altered T_g under hard confinement in terms of the competition in adsorbed layer between chain pinning and packing frustration, in which the former impedes chain mobility but the latter acts as additional free volume in the proximity to interface accordingly playing significant role in T_g reduction.[55,83,85] As such, the free volume holes diffusion (FVHD) model becomes a useful tool to describe the correlation between free volume in interface and the change of T_g, concluding that hard confinement on T_g does not merely depend on film thickness and interfacial interactions.[91,92] Correspondingly, Napolitano and coworkers indicated that adsorbed layer needs annealing time to form physiosorbed chains, and the ratio of adsorption time and the annealing time could be one explanation for the contradictive hard confinement effect on T_g.[83,93] Another explanation for these inconsistent results is the attractive interaction between the polymer and the hard confinement.[13,17,25,26,30,33,79,87] As a representative result, enhanced T_gs have been presented by PMMA or poly(2-vinylpyridine) (P2VP) thin films on silica substrate, as presented in Fig. 2, due to the hydrogen-bonding interaction between the polymers and silica.[13,17,26,30,33,79] Taking the opposite, for the interfaces lacking attractive interaction, T_g was found to be lower than the bulk value.[13,17,33] Furthermore, PS presented restrained T_g under confinement with interface of metallic oxide[55,73] or silica[17,21,75], whereas T_g of PS was improved with hard polymer confinement, such as PS thin films on PMMA[13,16] or polysulfone (PSF).[16] These results provide scientific insights for inconsistency of the hard confinement effect when the polymer or the hard confinement materials are different. Different interaction between polymer and confinement may induce reverse effect. However, some other results are in controversy, that is, deviation of T_g had opposite tendencies from the bulk value, even though the confinement system was organized by same polymer and similar hard confinements. Askar and coworkers found that T_g of PS in AAO was suppressed,[55,73] as opposed to the enhanced T_g of PS under same confinement reported by Wei and coworkers.[58,68] Thus, the mechanism of the confinement effects on T_g is remaining to be further revealed.

Effect on Physical Aging

Altered physical aging behavior caused from confinement is another major topic in last two decades. Although physical aging depends on the molecular mobility just as T_g, the mechanisms of hard confinement effects on them are different. For instance, Flory and coworkers found that the PMMA nanocomposite with unmodified single wall carbon nanotube (SWNT/PMMA) and amino-functionalized SWNT (a-SWNT/PMMA) showed different T_g variations compared to neat PMMA, namely invariant T_g for SWNT/PMMA and enhanced T_g for a-SWNT/PMMA, while their aging responses were both decelerated.[56] Moreover, some researchers devoted to investigating the decoupling between molecular dynamics and physical aging.[69–75,78] Boucher, Cangialosi, and their coworkers were focused on different properties measured by various methods, including segmental dynamics from broadband dielectric spectroscopy (BDS), structural parameter from the Tool-Narayanaswamy-Moynihan (TNM) model, and segmental relaxation time from thermally stimulated depolarization current (TSDC), to verify that hard confinement changes physical aging of nanocomposites while keeping the same molecular mechanism such as Havriliak-Negami (HN) relaxation compared to neat polymer, as presented in Fig. 3. They concluded that the physical aging under hard confinement not only depends on the molecular mobility but also the phenomenon can be well described by the FVHD model.

While positive correlation between hard confinement intensity and its effects on physical aging is widely accepted,[23,27,51,69–75,78] the unified theory of hard confinement effects on physical aging is not accomplished. Acce-

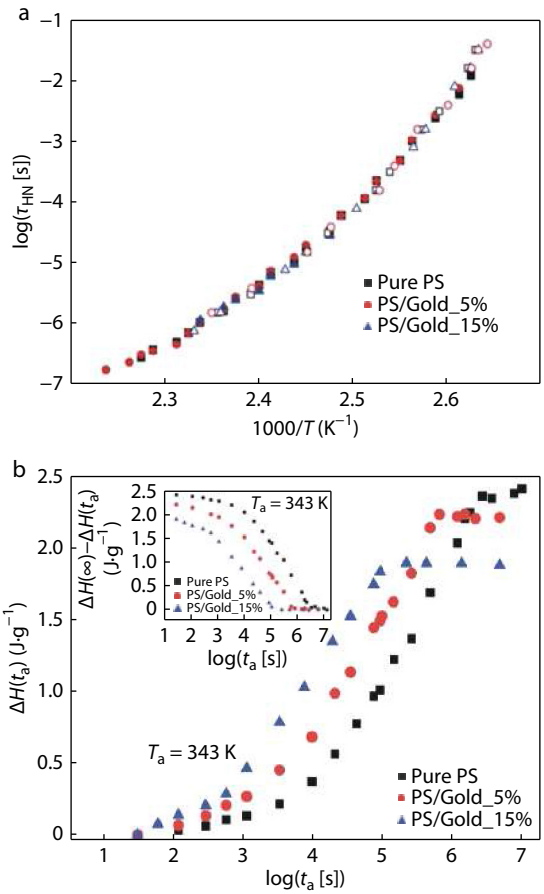

Fig. 3 Decoupling between molecular dynamics and physical aging. (a) Same HN relaxation time and (b) different enthalpy recovery for PS and PS/Gold nanocomposites. (Reprinted with permission from Ref. [73]; Copyright (2011) Royal Society of Chemistry).

lerated aging rate,[14,69–75,78,80] decelerated aging rate,[27,28,30,33,51,56,77,79,94] and invariant aging rate[58,77] to the bulk were demonstrated in different works. It should be noticed that the definitions of aging rate are different in different works using specific measuring methods. The aging rate can be usually defined by the time to reach equilibrium state, or the slope of the changed properties with respect to the logarithm of aging time. The mismatch of the definition of aging rate might be one reason for this inconsistency.[95]

Effect on Mechanical Properties

In last several decades, researchers made great efforts to explore suitable methods for directly investigating mechanical properties of polymers under nanoscale. As various methods emerge, influenced mechanical properties under nanoscale hard confinement were exposed. The main mechanical property staying focused is stiffness, on which the consensus is that moduli of polymers increase with increasing hard confinement intensity, as depicted in Fig. 4.[15,96–99] Similarly, the correlated mechanical properties, compliance were found reduced due to the hard confinement.[100] Hu and coworkers indicated that enhanced entanglement interaction at interface may be a reason for restrained polymer mobility, resulting in higher modulus.[97] In addition, interchain chemical bonds drove another argument for suppressed mobility.[98,101] For instance, Zheng and coworkers announced that the rotation and translation of polymer segmental in poly(vinyl acetate) (PVAc) thin films were impeded due to the polar hydrogen bonds between polymer and substrate with hydroxyl group, which increase modulus of PVAc thin films.[101]

Effect on Crystallization

Confinement effect on crystallization became a research hotspot in last two decades. It is found that several specifications of crystalline or semi-crystalline polymers, including nucleation,[102–115] crystal orientation,[103,105,107,109,110,116] crystallization rate,[103,108,112–115,117,118] and crystallization temperature (T_c) or melting temperature (T_m),[103,106,107,109,110,112,113,117] are altered due to hard confinement.

Instead of conventional heterogeneous nucleation in the crystallization of bulk polymers, the crystallization of polymers under hard confinement was reportedly dominated by homogeneous nucleation due to restricted mobility.[102–107,109,113] The homogenous nucleation is concomitant with compressed T_c.[103,104,106,107,109,110,112] Suzuki and coworkers presented a "phase diagram" to describe two nucleation regimes depending on proposed temperature and AAO hole curvature.[103] Homogeneous regime is close to glass state, whereas heterogeneous nucleation emerges at high temperature.[103] Accordingly, restrained T_c closed to T_g is regarded as an indicator for homogenous nucleation.[104,106] Moreover, hard confinement, especially hard nanoparticles, increases nucleation sites or nucleation density, resulting in higher crystallization rate with respect to bulk materials.[108,111,112,114,115] For example, Zhao and coworkers found that the nucleation efficiency of poly(ethylene oxide) (PEO) depends on their grafting density on SiO_2 nanoparticles in the composites.[108] They speculated that the energy barrier for nucleation may be disturbed or the sites for nucleation may be activated due to interfacial structures like loops or tails.[108] In addition, Strawhecker and coworkers reported higher nucleation density in sodium montmorillonite filled PEO, which is attributed to interrupted spatial continuity and restrained heterogeneous nucleation.[112]

The principal research of hard confinement effect on crystal orientation was carried upon AAO. In these works, crystal orientations parallel to[103,105–107,109,116] and perpendicular to[105,110] the AAO open channel coexist, depending on pore size of AAO and cooling rate. Steinhart and coworkers proposed the "kinetics selective growth" crystallization mechanism and indicated that chain axis is oriented perpendicular to pore direction for poly(vinylidene fluoride) (PVDF) confined in AAO.[116] Any crystal orientation with <*hkl*>* direction ($l \neq 0$) stops growing due to the confinement from channel walls.[116] After that, researchers systematically investigated crystal orientation of polymers in AAO and improved this mechanism. Su and coworkers reported that the fastest growth direction of PEO, *i.e.*, <120>*, is inclined to parallel to the AAO channel direction.[107] Guan and coworkers set a criterion to determine crystal orientation under confinement, that is, crystal growth is oriented parallel to the axis of the AAO channels when the pore diameter is greater than contour length of polymer chains *Nl*, while the crystals are aligned perpendicular to the channel axis when the pore dia-

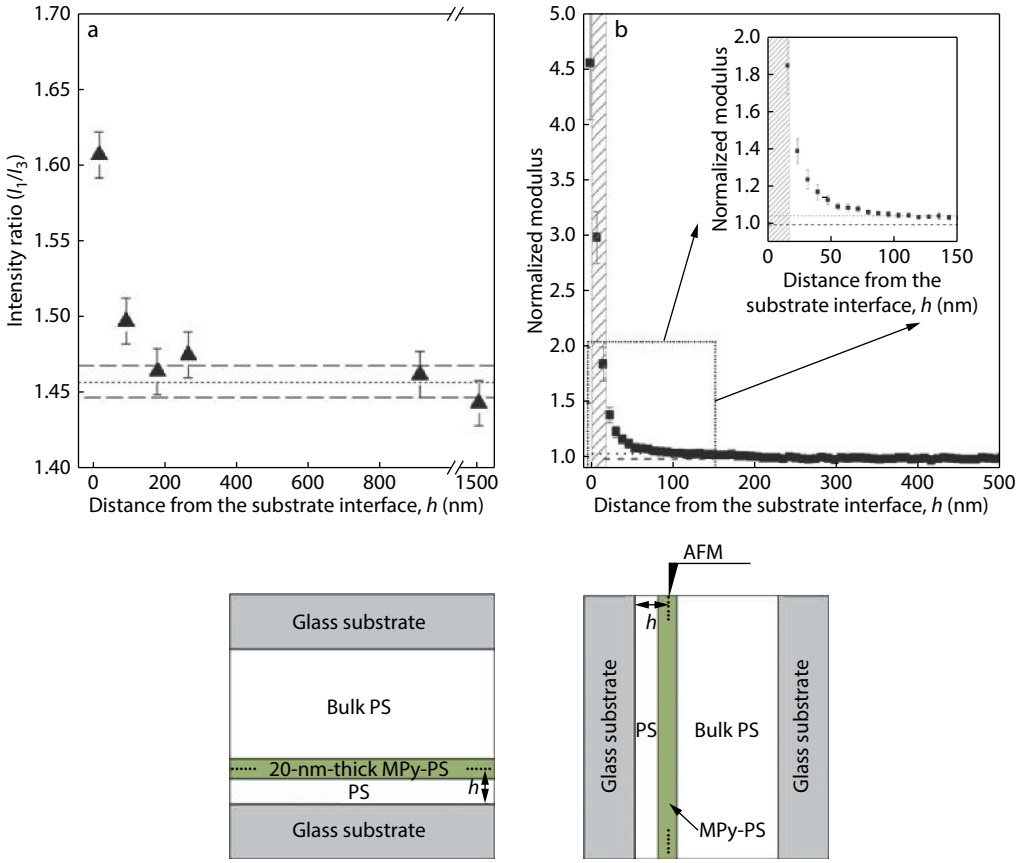

Fig. 4 (a) Intensity ratio and (b) normalized modulus as a function of the distance from the interface of PS and glass substrate. (Reprinted with permission from Ref. [99]; Copyright (2017) American Chemical Society).

meter is smaller than *NI*.[105] Furthermore, Su and coworkers depicted the dependence of cooling rate on crystal orientation, indicating three zones of orientation behavior of polymer confined in AAO. Thus, this work provided evidence showing that the "kinetics selective growth" mechanism would be invalid under specific conditions.[119]

The conclusions of hard confinement effect on crystallization rate are in controversy. That is, enhanced rate,[108,111,114,115,117] depressed rate or even completely suppressed crystallization,[103,112–114,117,118,120–122] are revealed in various works. In studies exploring the origins of these unmatched results, some publications showed that the interaction between polymer and hard confinement suppliers plays a crucial role in generating reduced chain mobility, which resulted in restrained crystallization.[118,121–124] However, Vanroy and coworkers suggested that suppressed crystallization kinetics of PET thin films confined between two adsorbing walls is ascribed to limited nuclei density instead of inhibited segmental mobility.[120] Kołodziejczyk and coworkers showed that hard confinement effect on crystallization rate depends on the pore size in AAO template.[117] Salol in AAO with pore size of 150 nm exhibited greater crystallization rate than the bulk. Nevertheless, with smaller pore size, crystallization is decelerated until being completely prohibited. Similar results were also presented by Dai *et al.* and Mijangos *et al.*[121,125] They found that the interfacial effect of AAO interrupts segmental mobility, while spatial heterogeneity enhances segmental mobility.[121,125,126] As such, interfacial effect increases but spatial heterogeneity reduces with decreasing pore size, resulting in inhibited crystallization of polymers in AAO compared to bulk materials.[121,125] Wu and coworker reported that temperature protocol is a noteworthy factor for the effect on crystallization rate.[114] In contrast to the restricted rate in cold crystallization (heating from room temperature to T_c), polylactide (PLA) composed with graphene displayed elevated rate in melt crystallization (cooling from high temperature to T_c) compared to neat PLA, as illustrated in Fig. 5.

It should be noticed that crystallization of polymer in AAO, including nucleation and growth process, may be substantially influenced by residual polymer on the surface of AAO template.[106,107,116] As such, future study of AAO confinement effect on crystallization should be extraordinarily careful to ensure experimental repeatability and reliability.

SOFT CONFINEMENT EFFECT

Effect on T_g

Different from inconsistent results for hard confinement effect on T_g, an amount of research had compatible conclusions for T_g under soft confinement, *i.e.*, reduced T_g with respect to the bulk value.[16,24,27,42–45,49,58,59,61–63,84,127–135] In these results, the relation between confinement intensity and magnitude of T_g deviation is consistent, showing that T_g decreases with increasing confinement intensity.[16,43–45,49,58,59,61–63,128,133–135] As

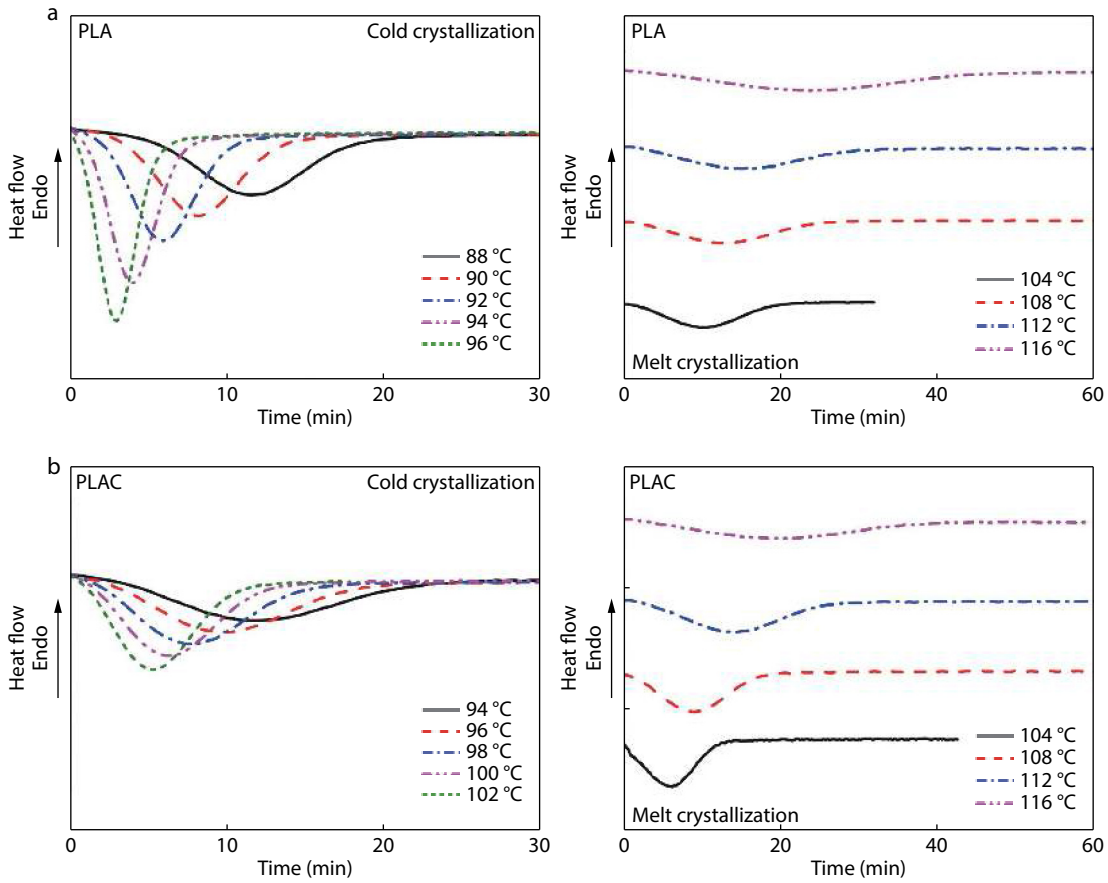

Fig. 5 Cold and melt crystallization for (a) neat PLA and (b) PLA/graphene composite, measured by differential scanning calorimetry. In experiments of melt crystallization, the sample was first heated up to 200 °C at a constant rate of 10 °C/min, and held thereafter for 5 min, and subsequently quenched to crystallization temperature at 80 °C/min, after that the exothermic heat flow as a function of time was recorded. To monitor the cold crystallization process, after melting at 200 °C for 5 min, the sample was first cooled to room temperature at 10 °C/min and then was rapidly heated to the crystallization temperature and annealed for isothermal crystallization. (Reprinted with permission from Ref. [114]; Copyright (2013) American Chemical Society).

described in Fig. 6, the soft poly(*n*-butyl methacrylate) (P*n*BMA) or poly(isobutyl methacrylate) (P*i*BMA) reduces T_g of PS in vicinity of the interface. In addition to confinement intensity, it is found that the magnitude of T_g reduction depends on materials' molecular weight.[42,133–135] The intrinsic size effect induces T_g reduction in low molecular weight regime, whereas it is dominated by chain confinement effects in high molecular weight regime.[134,135] It is widely accepted that the T_g reduction under soft confinement is attributed to the high mobility in the free surface.[63,129–132] For example, Zuo and coworkers found reduced T_g in poly(ethylene terephthalate) (PET) thin films, while these films exhibited same T_g as that of bulk materials after surface layer crystallizing.[132] Sharp and coworker showed suppressed T_g and invariant T_g in PS thin films with or without Al capping layer, respectively, compared to bulk T_g.[130] They also showed that restrained T_g could be recovered after removing Al capper, which gives a direct evidence to vital effect of free surface on T_g reduction regardless of sample preparation history.[130] Accordingly, researchers put great effort into investigation on the thickness of high mobility surface, which is determined to be 2–4 nm.[131,136–138] Although large numbers of works presented constrained T_g under soft confinement, a few opposite results still exist. For instance, T_g enhancement in PS nanoparticles or poly(bisphenol A carbonate) (PBAC) nanoparticles was reported by Martínez-Tong and coworkers.[60] They speculated that these enhanced T_gs should be attributed to the reduced number of conformational states in the nanoparticles constructed by few chains.

Effect on Physical Aging

A great number of works studying the soft confinement effect on physical aging showed that the aging of polymers was accelerated under soft confinement, compared to the bulk materials.[19,31,36–40,46,48,52,53,59,61] However, different conclusions, restricted or invariant aging, were detected in a few works.[27,44,52,53,58,80] In some of those results, the invariant aging was observed when soft confinement situations were constructed by relatively soft rubbers or the stacked films, as opposed to rapid aging of polymer with free surface.[44,52,53] Additionally, these systems may lack sufficient confinement intensity, as the stiffness discrepancy between rubber and the investigated polymers was not large enough and the stacked structure lost vast free surfaces presented in the single freestanding film. In recent years, it was argued that polymers could have a second fast equilibration mechanism, especially for

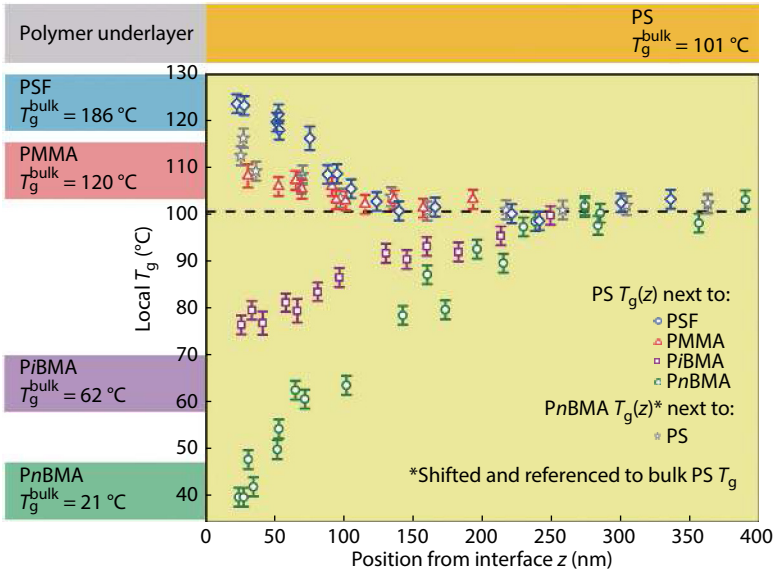

Fig. 6 T_g deviation of PS films on hard (PSF and PMMA) and soft (P*i*BMA and P*n*BMA) substrate with different distance *z* from the polymer-polymer interface. (Reprinted with permission from Ref. [16]; Copyright (2017) AIP Publishing).

polymers under soft confinement, in which the second mechanism emerges at short time scale.[36,37,61] Different time scales for the appearance of a fast equilibration mechanism might be a reason for incompatible soft confinement effect on physical aging. Though the conclusions of soft confinement effect on aging contain disagreement, the dependence of acceleration or deceleration on confinement intensity presented in these works is consistent, and the degree of aging rate deviation increases with enhanced confinement intensity.[27,36,38–41,59]

Effect on Mechanical Properties

The results of soft confinement effect on mechanical properties are more comprehensive and systematic, compared to the works on hard confinement effect, as the measurement systems for soft confinement are remarkably diverse. Existing breakthroughs in measurement of mechanical properties rely upon development of novel techniques, among which one recent progress is the determination of Young's modules *E*, from a buckling method,[50,139–142] or an ultrathin film tensile test,[143] or by capillary wrinkling.[144] In all of these measurements, ultrathin film must be in contact with a liquid or a soft substrate to form a bilayer system. The induced interfaces may be nontrivial in assessment of confinement effect on mechanical behavior of polymer films. Hence, the sample setup requirements restrict the generality of these novel techniques to be applied in a variety of scenarios. However, the diverse methods showed the inconsistent stiffness results of the soft confinement effect. Stiffness increase[139,144–146] or decrease[15,50,140–143] with increasing confinement intensity is reported in different works. Moreover, the confinement effects on strength including failure stress and strain are not quantitively consistent. Together with the findings above, it may indicate that the deep analysis and understanding on confinement influence on mechanical properties depend on the specific materials systems and the associated confinement conditions.[140,143,146,147] For example, Lee and coworker found that the fracture stress of PS decreases in thinner films, while the fracture strain becomes larger. In contrast, Yoon and coworkers reported enhanced rupture stress and reduced rupture strain of polyisobutylene (PIB) under soft confinement as illustrated in Fig. 7.[146]

Researchers devoted to expositing the physics of soft confinement on stiffness in last tens of years. It is found that the mechanical properties of polymers strongly depend on the entanglement of the polymer chains.[140,143,147] Thus, entanglement constraining polymer chain dynamics in different systems might be a crucial factor on the diverse soft confinement effects. Additionally, Torres and coworkers showed that the modulus of polymer with stiff backbones is independent of thickness, as opposed to constrained modulus with decreasing thickness in flexible polymer films, suggesting soft confinement effect on mechanical properties depending on main chain stiffness.[142] Another potential explanation is the competition between cohesive forces and the modulus of individual polymer chains. Page and coworkers suggested that the modulus of individual polymer chains plays a central role in the stiffness of thin films, as cohesive force is nonsignificant due to soft confinement. Thus, the modulus in thin films under soft confinement is enhanced with respect to bulk materials.[139]

Effect on Crystallization

The assorted morphologies formed by block copolymers are the most common situation to study soft confinement effect on crystallization, if the T_c of crystallized block is greater than the T_g of amorphous block. In last several decades, many efforts have been paid to studying such systems.[148–161] It is found that nucleation of polymer under soft confinement depends on confinement microdomain.[149,152,154,156,157,162] For lamella, heterogeneous nucleation is favored,[149,152,157,162] whereas the crystallization is controlled by homogeneous nucleation in cylindrical or spherical morphology.[152,156,157] Moreover, Ho and

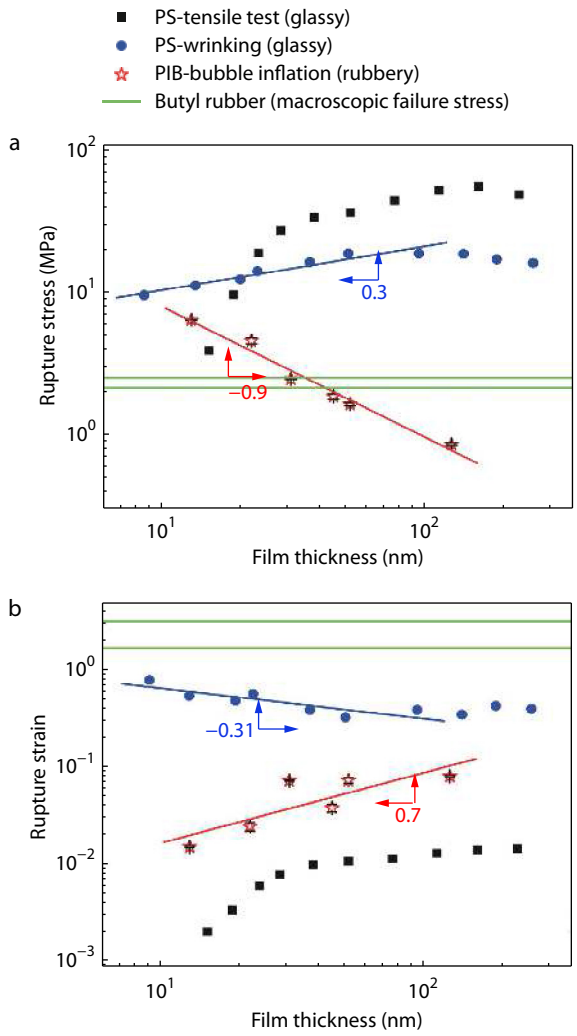

Fig. 7 Rupture (a) stress and (b) strain as a function of film thickness for PIB and PS thin films. (Reprinted with permission from Ref. [146]; Copyright (2017) American Chemical Society).

coworkers investigated crystallization of polystyrene-*b*-poly(L-lactide) (PS-*b*-PLLA) copolymer and first reported undulated morphology due to the transition from homogeneous to heterogeneous nucleation.[154] As same as nucleation, crystallization kinetics of polymers under soft confinement relies on confinement morphology. The first order Avrami kinetics for cylindrical or spherical confinement and spherulitic crystallization for lamella were validated in many works.[149,152,156,157] Unfortunately, the results of soft confinement on crystallization rate did not show good consistency: reduced[148–150] or enhanced crystallization rate[162] was reported in different works.

DISCUSSION

Examining the results shown above, materials under soft confinement show more compatible conclusions than those under hard confinement. Moreover, several works have succeeded in predicting the soft confinement effect by different models. For instance, Tito, DeFelice and their coworkers offered a limited mobility model to simulate free volume and mobility.[163,164] They found that mobility of polymer films directly contacted with high mobility materials was clearly enhanced. The enhanced mobility reduces the T_g of polymer films with free surface. Lang and coworkers utilized the dependence of interfacial adhesion energy to perform the T_g suppression under soft confinement.[165] These models provide valuable tools to describe and understand the soft confinement effects.

It has been indicated that stress has a great impact on aging rate in supported films or free-standing films with circular opening holder.[19,29] As such, the different results of confinement effect on physical aging might be attributed to mismatched thermal expansion between polymer and confinement provider, which introduces additional stress in aging process.

The hard confinement systems are complicated if the free surfaces are involved in the systems. In most cases, soft and hard confinements are co-existent, especially for a thin film supported on a hard substrate. The measured confinement effects reflect the overall interplay between the soft and hard confinement, relying on the ratio of two confinement intensities. The stronger confinement dominates the overall effect in these systems. For instance, the PMMA nanolines on silica showed reduced T_g due to the high free-surface-to-interface ratio, in opposition to the enhanced T_g of the PMMA thin films on silica, as displayed in Fig. 8.[24] The competition between hard and soft confinements may be one of the reasons for the inconsistency of confinement effect in some similar systems but having different confinement intensities. Similar systems, even constructed by same polymer and same confinement materials, can perform considerably different effects due to the discrepant fraction of free surface. Moreover, the compet-

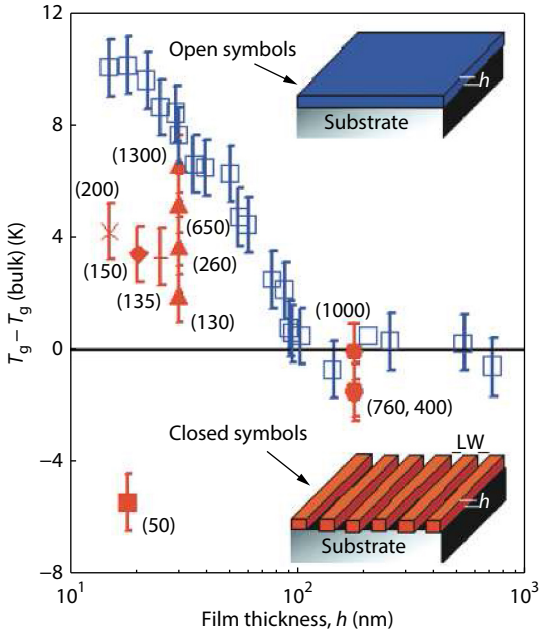

Fig. 8 Different free-surface-to-interface ratio induced T_g deviation of PMMA films (open squares) and nanolines with thickness of 175 nm (●), 30 nm (▲), 25 nm (┼), 20 nm (◆), 18 nm (■), and 15 nm (×), respectively. The numbers in parentheses specify the line widths. (Reprinted with permission from Ref. [24]; Copyright (2007) American Chemical Society).

https://doi.org/10.1007/s10118-020-2380-3

ition can be used to explain the invariant effects results after changing the confinement condition.[13,31] For example, Roth and coworkers found that the T_g of P2VP thin films on silica substrate remained elevated as ever after capped with PS layer, as the confinement induced by silica substrate was much stronger than the confinement provided by PS layer atop or the free surface.[13] Consequently, the inconsistency of hard confinement effect on T_g or physical aging may be attributed to the complexity of confinement systems. In order to reduce the complexity of system and avoid the impact from free surface, fluorescence measurements are considered as an ideal technology in studies of thin films supported on substrate. A thick layer above the labeled thin films can impede the effects of free surface.

The transformation between soft and hard confinement will bring complexity as well, especially in the investigation of crystallization in block copolymers.[166–171] For instance, during the crystallization of PEO blocks in PEO-PS block copolymer with microphase separation,[166–169,171] PS blocks form hard confinement to PEO blocks at the beginning of crystallization due to the lower stiffness of PEO blocks. However, with the crystallization progressing, the PEO crystals become harder than the amorphous PS. Consequently, the confinement provided by PS blocks shifts from hard to soft, with respect to PEO crystallization process.

In addition to the apparent confinement effects, the confinement systems are even more remarkable if utilizing the system as a tool to study some extreme or inaccessible states on experimental timescale. Upon the rapid aging induced by soft confinement, Boucher, Perez-De-Eulate and coworkers found evidence for existence of the two mechanisms of physical aging equilibrium that are impossible to achieve in such short time for bulk materials.[36,37,61] Moreover, Boucher and coworker found that the fictive temperature of PS reached the predicted Kauzmann temperature (T_K) in two days under soft confinement as demonstrated in Fig. 9.[37] The results are significant since the experimental evidence of the thermodynamic (ideal) glass transition is unprecedented to our knowledge, as more than millions of years are necessary to reach T_K for bulk materials.

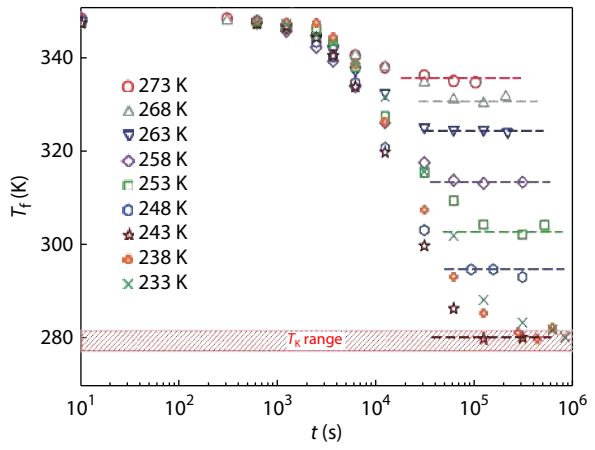

Fig. 9 Fictive temperature as a function of aging time for different aging temperatures. (Reprinted with permission from Ref. [37]; Copyright (2017) Royal Society of Chemistry).

CONCLUSIONS

This review highlights classic and novel methods for making soft or hand confinements in 1D, 2D and 3D systems. The polymers have substantially different properties under confinement, compared to the bulk materials. The effect of soft and hard confinements on four major themes, glass transition temperature, physical aging, mechanical properties, and crystallization are reviewed in details. Most of the existing works show good consistency in the results of suppressed T_g under soft confinement, while the hard confinement effect on T_g needs further efforts to attain scientific insight and systematic conclusion due to the complexity induced by various interactions between the materials. The confinement effects on physical aging do not have consistent results, partially due to the fact that the definitions of aging rate are not the same in different works. Soft confinement effects on stiffness are in controversy just as on strength due to multiplex measure methods. In contrast, the results of effect of hard confinement are identical. Whereas it is indicated that hard confinement induces homogenous nucleation and reduced T_c and T_m, the effect of hard confinement on crystallization rate still causes dispute. Fortunately, crystal orientation of polymers in AAO has been well depicted by mature mechanism, depending on pore size of AAO and cooling rate. Soft confinement effect on crystallization, including nucleation and crystallization kinetics, principally relies on confinement microdomain. Although the mechanism of confinement effect on segmental motion has not been elucidated clearly, confinement systems are useful in studying the glass transition or physical aging. Comparing to the bulk, it is easier to make polymeric materials with confinement reaching some extreme conditions in short time scale due to the accelerated aging.

ACKNOWLEDGMENTS

The authors acknowledge the National Natural Science Foundation of China for financial support through the General Program No. 2157408. Y.G. is very grateful to the National Youth 1000 Talent Program of China, the Shanghai 1000 Talent Plan, and the support by the Scientific Research Foundation for the Returned Overseas Chinese Scholars, State Education Ministry of China. The authors also acknowledge the start-up fund of Y.G. from both University of Michigan-Shanghai Jiao Tong University Joint Institute, and School of Materials Science and Engineering at SJTU.

REFERENCES

1 Frieberg, B.; Glynos, E.; Sakellariou, G.; Green, P. F. Physical aging of star-shaped macromolecules. *ACS Macro Lett.* **2012**, *1*, 636–640.
2 Simon, S. L.; Plazek, D. J.; Sobieski, J. W.; Mcgregor, E. T. Physical aging of a polyetherimide: volume recovery and its comparison to creep and enthalpy meas. *J. Polym. Sci., Part B: Polym. Phys.* **1997**, *35*, 929–936.
3 Huang, Y.; Wang, X.; Paul, D. R. Physical aging of thin glassy polymer films: free volume interpretation. *J. Membr. Sci.* **2006**, *277*, 219–229.
4 Cowie, J. M. G.; Ferguson, R. Physical aging studies in poly(vinyl

methyl ether). 1. Enthalpy relaxation as a function of aging temperature. *Macromolecules* **1989**, *22*, 2307–2312.
5 Cowie, J. M. G.; Harris, S.; McEwen, I. J. Physical aging in poly(vinyl acetate). 2. Relative rates of volume and enthalpy relaxation. *Macromolecules* **1998**, *31*, 2611–2615.
6 Odegard, G. M.; Bandyopadhyay, A. Physical aging of epoxy polymers and their composites. *J. Polym. Sci., Part B: Polym. Phys.* **2011**, *49*, 1695–1716.
7 Low, Z. X.; Budd, P. M.; McKeown, N. B.; Patterson, D. A. Gas permeation properties, physical aging, and its mitigation in high free volume glassy polymers. *Chem. Rev.* **2018**, *118*, 5871–5911.
8 Swaidan, R.; Ghanem, B.; Litwiller, E.; Pinnau, I. Physical aging, plasticization and their effects on gas permeation in "rigid" polymers of intrinsic microporosity. *Macromolecules* **2015**, *48*, 6553–6561.
9 Ma, X.; Pinnau, I. Effect of film thickness and physical aging on "intrisic" gas permeation properties of microporous ethanoanthracene-based polyimides. *Macromolecules* **2018**, *51*, 1069–1076.
10 Hutchinson, J. M. Physical aging of polymers. *Prog. Polym. Sci.* **1995**, *20*, 703–760.
11 Roe, R. J.; Millman, G. M. Physical aging in polystyrene: comparison of the changes in creep behavior with the enthalpy relaxation. *Polym. Eng. Sci.* **1983**, *23*, 318–322.
12 Soloukhin, V. A.; Brokken-Zijp, J. M.; Asselen, O. L. J. V.; With, G. D. Physical aging of polycarbonate: elastic modulus, hardness, creep, endothermic peak, molecular weight distribution, and infrared data. *Macromolecules* **2003**, *36*, 7585–7597.
13 Roth, C. B.; McNerny, K. L.; Jager, W. F.; Torkelson, J. M. Eliminating the enhanced mobility at the free surface of polystyrene: fluorescence studies of the glass transition temperature in thin bilayer films of immiscible polymers. *Macromolecules* **2007**, *40*, 2568–2574.
14 Ma, M.; Guo, Y. Accelerated aging of PS blocks in PS-*b*-PMMA diblock copolymer under hard confinement. *J. Phys. Chem. B* **2019**, *123*, 2448–2453.
15 Askar, S.; Torkelson, J. M. Stiffness of thin, supported polystyrene films: free-surface, substrate, and confinement effects characterized *via* self-referencing fluorescence. *Polymer* **2016**, *99*, 417–426.
16 Baglay, R. R.; Roth, C. B. Local glass transition temperature $T_g(z)$ of polystyrene next to different polymers: hard vs. soft confinement. *J. Chem. Phys.* **2017**, *146*, 203307.
17 Ellison, C. J.; Kim, S. D.; Hall, D. B.; Torkelson, J. M. Confinement and processing effects on glass transition temperature and physical aging in ultrathin polymer films: novel fluorescence measurements. *Eur. Phys. J. E: Soft Matter Biol. Phys.* **2002**, *8*, 155–166.
18 Glor, E. C.; Fakhraai, Z. Facilitation of interfacial dynamics in entangled polymer films. *J. Chem. Phys.* **2014**, *141*, 194505.
19 Gray, L. A. G.; Yoon, S. W.; Pahner, W. A.; Davidheiser, J. E.; Roth, C. B. Importance of quench conditions on the subsequent physical aging rate of glassy polymer films. *Macromolecules* **2012**, *45*, 1701–1709.
20 Horn, N. R.; Paul, D. R. Carbon dioxide sorption and plasticization of thin glassy polymer films tracked by optical methods. *Macromolecules* **2012**, *45*, 2820–2834.
21 Keddie, J. L.; Jones, R. A. L.; Cory, R. A. Size-dependent depression of the glass transition temperature in polymer films. *Europhys. Lett.* **1994**, *27*, 59–64.
22 Kipnusu, W. K.; Elsayed, M.; Krause-Rehberg, R.; Kremer, F. Glassy dynamics of polymethylphenylsiloxane in one- and two-dimensional nanometric confinement—a comparison. *J. Chem. Phys.* **2017**, *146*, 203302.
23 Kushner, D. I.; Hickner, M. A. Substrate-dependent physical aging of confined nafion thin films. *ACS Macro Lett.* **2018**, *7*, 223–227.
24 Mundra, M. K.; Donthu, S. K.; Dravid, V. P.; Torkelson, J. M. Effect of spatial confinement on the glass-transition temperature of patterned polymer nanostructures. *Nano Lett.* **2007**, *7*, 713–718.
25 Mundra, M. K.; Ellison, C. J.; Rittigstein, P.; Torkelson, J. M. Fluorescence studies of confinement in polymer films and nanocomposites: glass transition temperature, plasticizer effects, and sensitivity to stress relaxation and local polarity. *Eur. Phys. J. Special Topics* **2007**, *141*, 143–151.
26 Priestley, R. D.; Broadbelt, L. J.; Torkelson, J. M. Physical aging of ultrathin polymer films above and below the bulk glass transition temperature: effects of attractive vs neutral polymer-substrate interactions measured by fluorescence. *Macromolecules* **2005**, *38*, 654–657.
27 Priestley, R. D.; Ellison, C. J.; Broadbelt, L. J.; Torkelson, J. M. Structural relaxation of polymer glasses at surfaces, interfaces, and in between. *Science* **2005**, *309*, 456–459.
28 Pye, J. E.; Rohald, K. A.; Baker, E. A.; Roth, C. B. Physical aging in ultrathin polystyrene films: evidence of a gradient in dynamics at the free surface and its connection to the glass transition temperature reductions. *Macromolecules* **2010**, *43*, 8296–8303.
29 Pye, J. E.; Roth, C. B. Physical aging of polymer films quenched and measured free-standing *via* ellipsometry: controlling stress imparted by thermal expansion mismatch between film and support. *Macromolecules* **2013**, *46*, 9455–9463.
30 Rittigstein, P.; Priestley, R. D.; Broadbelt, L. J.; Torkelson, J. M. Model polymer nanocomposites provide an understanding of confinement effects in real nanocomposites. *Nat. Mater.* **2007**, *6*, 278–282.
31 Rowe, B. W.; Pas, S. J.; Hill, A. J.; Suzuki, R.; Freeman, B. D.; Paul, D. R. A variable energy positron annihilation lifetime spectroscopy study of physical aging in thin glassy polymer films. *Polymer* **2009**, *50*, 6149–6156.
32 Sharma, R. P.; Green, P. F. Role of "hard" and "soft" confinement on polymer dynamics at the nanoscale. *ACS Macro Lett.* **2017**, *6*, 908–914.
33 Torkelson, J. M.; Priestley, R. D.; Rittigstein, P.; Mundra, M. K.; Roth, C. B. Novel effects of confinement and interfaces on the glass transition temperature and physical aging in polymer films and nanocomposites. *AIP Conf. Proc.* **2008**, *982*, 192.
34 Yavari, M.; Maruf, S.; Ding, Y.; Lin, H. Physical aging of glassy perfluoropolymers in thin film composite membranes. Part II. Glass transition temperature and the free volume model. *J. Membr. Sci.* **2017**, *525*, 399–408.
35 Yavari, M.; Le, T.; Lin, H. Physical aging of glassy perfluoropolymers in thin film composite membranes. Part I. Gas transport properties. *J. Membr. Sci.* **2017**, *525*, 387–398.
36 Boucher, V. M.; Cangialosi, D.; Alegría, A. Complex nonequilibrium dynamics of stacked polystyrene films deep in the glassy state. *J. Chem. Phys.* **2017**, *146*, 203312.
37 Boucher, V. M.; Cangialosi, D.; Alegría, A.; Colmenero, J. Reaching the ideal glass transition by aging polymer films. *Phys. Chem. Chem. Phys.* **2017**, *19*, 961–965.
38 Dorkenoo, K. D.; Pfromm, P. H. Accelerated physical aging of thin poly[1-(trimethylsilyl)-1-propyne] films. *Macromolecules* **2000**, *33*, 3747–3751.
39 Huang, Y.; Paul, D. R. Physical aging of thin glassy polymer films monitored by optical properties. *Macromolecules* **2006**, *39*, 1554–1559.
40 Huang, Y.; Paul, D. R. Effect of film thickness on the gas-permeation characteristics of glassy polymer membranes. *Ind. Eng. Chem. Res.* **2007**, *46*, 2342–2347.

https://doi.org/10.1007/s10118-020-2380-3

41 Huang, Y.; Paul, D. R. Effect of molecular weight and temperature on physical aging of thin glassy poly(2,6-dimethyl-1,4-phenylene oxide) films. *J. Polym. Sci., Part B: Polym. Phys.* **2007**, *45*, 1390–1398.

42 Kim, S.; Roth, C. B.; Torkelson, J. M. Effect of nanoscale confinement on the glass transition temperature of free-standing polymer films: novel, self-referencing fluorescence method. *J. Polym. Sci., Part B: Polym. Phys.* **2008**, *46*, 2754–2764.

43 Koh, Y. P.; Mckenna, G. B.; Simon, S. L. Calorimetric glass transition temperature and absolute heat capacity of polystyrene ultrathin films. *J. Polym. Sci., Part B: Polym. Phys.* **2006**, *44*, 3518–3527.

44 Koh, Y. P.; Simon, S. L. Structural relaxation of stacked ultrathin polystyrene films. *J. Polym. Sci., Part B: Polym. Phys.* **2008**, *46*, 2741–2753.

45 Pye, J. E.; Roth, C. B. Two simultaneous mechanisms causing glass transition temperature reductions in high molecular weight freestanding polymer films as measured by transmission ellipsometry. *Phys. Rev. Lett.* **2011**, *107*, 235701.

46 Rowe, B. W.; Freeman, B. D.; Paul, D. R. Physical aging of ultrathin glassy polymer films tracked by gas permeability. *Polymer* **2009**, *50*, 5565–5575.

47 Akhrass, S. A.; Reiter, G.; Hou, S. Y.; Yang, M. H.; Chang, Y. L.; Chang, F. C.; Wang, C. F.; Yang, A. C. M. Viscoelastic thin polymer films under transient residual stresses: two-stage dewetting on soft substrates. *Phys. Rev. Lett.* **2008**, *100*, 178301.

48 Murphy, T. M.; Freeman, B. D.; Paul, D. R. Physical aging of polystyrene films tracked by gas permeability. *Polymer* **2013**, *54*, 873–880.

49 Rauscher, P. M.; Pye, J. E.; Baglay, R. R.; Roth, C. B. Effect of adjacent rubbery layers on the physical aging of glassy polymers. *Macromolecules* **2013**, *46*, 9806–9817.

50 Stafford, C. M.; Vogt, B. D.; Harrison, C.; Julthongpiput, D.; Huang, R. Elastic moduli of ultrathin amorphous polymer films. *Macromolecules* **2006**, *39*, 5095–5099.

51 Langhe, D. S.; Murphy, T. M.; Shaver, A.; LaPorte, C.; Freeman, B. D.; Paul, D. R.; Baer, E. Structural relaxation of polystyrene in nanolayer confinement. *Polymer* **2012**, *53*, 1925–1931.

52 Murphy, T. M.; Langhe, D. S.; Ponting, M.; Baer, E.; Freeman, B. D.; Paul, D. R. Physical aging of layered glassy polymer films *via* gas permeability tracking. *Polymer* **2011**, *52*, 6117–6125.

53 Murphy, T. M.; Langhe, D. S.; Ponting, M.; Baer, E.; Freeman, B. D.; Paul, D. R. Enthalpy recovery and structural relaxation in layered glassy polymer films. *Polymer* **2012**, *53*, 4002–4009.

54 Mueller, C. D.; Nazarenko, S.; Ebeling, T.; Schuman, T. L.; Hiltner, A.; Baer, E. Novel structures by microlayer coextrusion-talc-filled PP, PC/SAN, and HDPE/LLDPE. *Polym. Eng. Sci.* **1997**, *37*, 355–362.

55 Askar, S.; Wei, T.; Tan, A. W.; Torkelson, J. M. Molecular weight dependence of the intrinsic size effect on T_g in AAO template-supported polymer nanorods: a DSC study. *J. Chem. Phys.* **2017**, *146*, 203323.

56 Flory, A. L.; Ramanathan, T.; Brinson, L. C. Physical aging of single wall carbon nanotube polymer nanocomposites: effect of functionalization of the nanotube on the enthalpy relaxation. *Macromolecules* **2010**, *43*, 4247–4252.

57 Teng, C.; Li, L.; Wang, Y.; Wang, R.; Chen, W.; Wang, X.; Xue, G. How thermal stress alters the confinement of polymers vitrificated in nanopores. *J. Chem. Phys.* **2017**, *146*, 203319.

58 Wei, W.; Feng, S.; Zhou, Q.; Liang, H.; Long, Y.; Wu, Q.; Gao, H.; Liang, G.; Zhu, F. Study on glass transition and physical aging of polystyrene nanowires by differential scanning calorimetry. *J. Polym. Res.* **2017**, *24*, 38.

59 Guo, Y.; Zhang, C.; Lai, C.; Priestley, R. D.; D'Acunzi, M.; Fytas, G. Structural relaxation of polymer nanospheres under soft and hard confinement: isobaric versus isochoric conditions. *ACS Nano* **2011**, *5*, 5365–5373.

60 Martínez-Tong, D. E.; Cui, J.; Soccio, M.; García, C.; Ezquerra, T. A.; Nogales, A. Does the glass transition of polymers change upon 3D confinement? *Macromol. Chem. Phys.* **2014**, *215*, 1620–1624.

61 Perez-De-Eulate, N. G.; Cangialosi, D. Double mechanism for structural recovery of polystyrene nanospheres. *Macromolecules* **2018**, *51*, 3299–3307.

62 Zhang, C.; Boucher, V. M.; Cangialosi, D.; Priestley, R. D. Mobility and glass transition temperature of polymer nanospheres. *Polymer* **2013**, *54*, 230–235.

63 Zhang, C.; Guo, Y.; Priestley, R. D. Glass transition temperature of polymer nanoparticles under soft and hard confinement. *Macromolecules* **2011**, *44*, 4001–4006.

64 Zhang, C.; Guo, Y.; Shepard, K. B.; Priestley, R. D. Fragility of an isochorically confined polymer glass. *J. Phys. Chem. Lett.* **2013**, *4*, 431–436.

65 Zhang, L.; D'Acunzi, M.; Kappl, M.; Auernhammer, G. K.; Vollmer, D. Hollow silica spheres: synthesis and mechanical properties. *Langmuir* **2009**, *25*, 2711–2717.

66 Zhang, C.; Pansare, V. J.; Prud'homme, R. K.; Priestley, R. D. Flash nanoprecipitation of polystyrene nanoparticles. *Soft Matter* **2012**, *8*, 86–93.

67 Graf, C.; Vossen, D. L. J.; Imhof, A.; Blaaderen, A. V. A general method to coat colloidal particles with silica. *Langmuir* **2003**, *19*, 6693–6700.

68 Zhu, L.; Wang, X.; Gu, Q.; Chen, W.; Sun, P.; Xue, G. Confinement-induced deviation of chain mobility and glass transition temperature for polystyrene/Au nanoparticles. *Macromolecules* **2013**, *46*, 2292–2297.

69 Boucher, V. M.; Cangialosi, D.; Alegría, A.; Colmenero, J. Enthalpy recovery of PMMA/silica nanocomposites. *Macromolecules* **2010**, *43*, 7594–7603.

70 Boucher, V. M.; Cangialosi, D.; Alegría, A.; Colmenero, J. Time dependence of the segmental relaxation time of poly(vinyl acetate)-silica nanocomposites. *Phys. Rev. E* **2012**, *86*, 041501.

71 Boucher, V. M.; Cangialosi, D.; Alegría, A.; Colmenero, J.; González-Irun, J.; Liz-Marzan, L. M. Accelerated physical aging in PMMA/silica nanocomposites. *Soft Matter* **2010**, *6*, 3306–3317.

72 Boucher, V. M.; Cangialosi, D.; Alegrìa, A.; Colmenero, J.; González-Irun, J.; Liz-Marzan, L. M. Physical aging in PMMA/silica nanocomposites: enthalpy and dielectric relaxation. *J. Non-Cryst. Solids* **2011**, *357*, 605–609.

73 Boucher, V. M.; Cangialosi, D.; Alegría, A.; Colmenero, J.; Pastoriza-Santos, I.; Liz-Marzan, L. M. Physical aging of polystyrene/gold nanocomposites and its relation to the calorimetric T_g depression. *Soft Matter* **2011**, *7*, 3607–3620.

74 Cangialosi, D.; Boucher, V. M.; Alegría, A.; Colmenero, J. Free volume holes diffusion to describe physical aging in poly(mehtyl methacrylate)/silica nanocomposites. *J. Chem. Phys.* **2011**, *135*, 014901.

75 Cangialosi, D.; Boucher, V. M.; Alegría, A.; Colmenero, J. Enhanced physical aging of polymer nanocomposites: the key role of the area to volume ratio. *Polymer* **2012**, *53*, 1362–1372.

76 Koerner, H.; Opsitnick, E.; Grabowski, C. A.; Drummy, L. F.; Hsiao, M. S.; Che, J.; Pike, M.; Person, V.; Bockstaller, M. R.; Meth, J. S.; Vaia, R. A. Physical aging and glass transition of hairy nanoparticle assemblies. *J. Polym. Sci., Part B: Polym. Phys.* **2016**, *54*, 319–330.

77 Priestley, R. D.; Rittigstein, P.; Broadbelt, L. J.; Fukao, K.; Torkelson, J. M. Evidence for the molecular-scale origin of the suppression of physical ageing in confined polymer: fluorescence and dielectric spectroscopy studies of polymer-silica nanocomposites. *J. Phys.: Condens. Matter* **2007**, *19*, 205120.

https://doi.org/10.1007/s10118-020-2380-3

78 Ramakrishnan, V.; Harsiny, S.; Goossens, J. G. P.; Hoeks, T. L.; Peters, G. W. M. Physical aging in polycarbonate nanocomposites containing grafted nanosilica particles: a comparison between enthalpy and yield stress evolution. *J. Polym. Sci., Part B: Polym. Phys.* **2016**, *54*, 2069–2081.
79 Rittigstein, P.; Torkelson, J. M. Polymer-nanoparticle interfacial interactions in polymer nanocomposites: confinement effects on glass transition temperature and suppression of physical aging. *J. Polym. Sci., Part B: Polym. Phys.* **2006**, *44*, 2935–2943.
80 Ma, M.; Huang, Y.; Guo, Y. Enthalpy relaxation and morphology evolution in polystyrene-*b*-poly(methyl methacrylate) diblock copolymer. *Macromolecules* **2018**, *51*, 7368–7376.
81 Ma, M.; Xue, T.; Chen, S.; Guo, Y.; Chen, Y.; Liu, H. Features of structural relaxation in diblock copolymers. *Polym. Test.* **2017**, *60*, 1–5.
82 Yin, H.; Napolitano, S.; Schönhals, A. Molecular mobility and glass transition of thin films of poly(bisphenol A carbonate). *Macromolecules* **2012**, *45*, 4652–4662.
83 Rotella, C.; Napolitano, S.; Cremer, L. D.; Koeckelberghs, G.; Wübbenhorst, M. Distribution of segmental mobility in ultrathin polymer films. *Macromolecules* **2010**, *43*, 8686–8691.
84 Forrest, J. A.; Svanberg, C.; Révész, K.; Rodahl, M.; Torell, L. M.; Kasemo, B. Relaxation dynamics in ultrathin polymer films. *Phys. Rev. E* **1998**, *58*, 1226–1229.
85 Napolitano, S.; Pilleri, A.; Rolla, P.; Wübbenhorst, M. Unusual deviations from bulk behavior in ultrathin films of poly(*tert*-butylstyrene): can dead layers induce a reduction of T_g? *ACS Nano* **2010**, *4*, 841–848.
86 Sun, S.; Xu, H.; Han, J.; Zhu, Y.; Zuo, B.; Wang, X.; Zhang, W. The architecture of the adsorbed layer at the substrate interface determines the glass transition of supported ultrathin polystyrene films. *Soft Matter* **2016**, *12*, 8348–8358.
87 Sharp, J. S.; Forrest, J. A. Dielectric and ellipsometric studies of the dynamics in thin films of isotactic poly(methylmethacrylate) with one free surface. *Phys. Rev. E* **2003**, *67*, 031805.
88 Fakhraai, Z.; Forrest, J. A. Probing slow dynamics in supported thin polymer films. *Phys. Rev. Lett.* **2005**, *95*, 025701.
89 Napolitano, S.; Wübbenhorst, M. Dielectric signature of a dead layer in ultrathin films of a nonpolar polymer. *J. Phys. Chem. B* **2007**, *111*, 9197–9199.
90 Napolitano, S.; Lupaşcu, V.; Wübbenhorst, M. Temperature dependence of the deviations from bulk behavior in ultrathin polymer films. *Macromolecules* **2008**, *41*, 1061–1063.
91 Napolitano, S.; Cangialosi, D. Interfacial free volume and vitrification: reduction in T_g in proximity of an adsorbing interface explained by the free volume holes diffusion model. *Macromolecules* **2013**, *46*, 8051–8053.
92 Napolitano, S.; Rotella, C.; Wübbenhorst, M. Can thickness and interfacial interactions univocally determine the behavior of polymers confined at the nanoscale? *ACS Macro Lett.* **2012**, *1*, 1189–1193.
93 Napolitano, S.; Wübbenhorst, M. The lifetime of the deviations from bulk behaviour in polymers confined at the nanoscale. *Nat. Commun.* **2011**, *2*, 260.
94 Napolitano, S.; Prevosto, D.; Lucchesi, M.; Pingue, P.; D'Acunto, M.; Rolla, P. Influence of a reduced mobility layer on the structural relaxation dynamics of aluminum capped ultrathin films of poly(ethylene terephthalate). *Langmuir* **2007**, *23*, 2103–2109.
95 Cangialosi, D.; Boucher, V. M.; Alegría, A.; Colmenero, J. Physical aging in polymers and polymer nanocomposites: recent results and open questions. *Soft Matter* **2013**, *9*, 8619–8630.
96 Cheng, X.; Putz, K. W.; Wood, C. D.; Brinson, L. C. Characterization of local elastic modulus in confined polymer films *via* AFM indentation. *Macromol. Rapid Commun.* **2015**, *36*, 391–397.
97 Hu, H. W.; Granick, S. Viscoelastic dynamics of confined polymer melts. *Science* **1992**, *258*, 1339–1342.
98 Li, L.; Alsharif, N.; Brown, K. A. Confinement-induced stiffening of elastomer thin films. *J. Phys. Chem. B* **2018**, *122*, 10767–10773.
99 Zhang, M.; Askar, S.; Torkelson, J. M.; Brinson, L. C. Stiffness gradients in glassy polymer model nanocomposites: comparisons of quantitative characterization by fluorescence spectroscopy and atomic force microscopy. *Macromolecules* **2017**, *50*, 5447–5458.
100 O'Connell, P. A.; McKenna, G. B. Rheological measurements of the thermoviscoelastic response of ultrathin polymer films. *Science* **2005**, *307*, 1760–1763.
101 Zheng, F.; Zuo, B.; Zhu, Y.; Yang, J.; Wang, X. Probing substrate effects on relaxation dynamics of ultrathin poly(vinyl acetate) films by dynamic wetting of water droplets on their surfaces. *Soft Matter* **2013**, *9*, 11680–11689.
102 Nakagawa, S.; Tanaka, T.; Ishizone, T.; Nojima, S.; Kamimura, K.; Yamaguchi, K.; Nakahama, S. Crystallization behavior of poly(ε-caprolactone) chains confined in lamellar nanodomains. *Polymer* **2014**, *55*, 4394–4400.
103 Suzuki, Y.; Duran, H.; Steinhart, M.; Butt, H. J. R.; Floudas, G. Suppression of poly(ethylene oxide) crystallization in diblock copolymers of poly(ethylene oxide)-*b*-poly(ε-caprolactone) confined to nanoporous alumina. *Macromolecules* **2014**, *47*, 1793–1800.
104 Wen, X.; Su, Y.; Shui, Y.; Zhao, W.; Müller, A. J.; Wang, D. Correlation between grafting density and confined crystallization behavior of poly(ethylene glycol) grafted to silica. *Macromolecules* **2019**, *52*, 1505–1516.
105 Guan, Y.; Liu, G.; Gao, P.; Li, L.; Ding, G.; Wang, D. Manipulating crystal orientation of poly(ethylene oxide) by nanopores. *ACS Macro Lett.* **2013**, *2*, 181–184.
106 Shi, G.; Liu, G.; Su, C.; Chen, H.; Chen, Y.; Su, Y.; Müller, A. J.; Wang, D. Reexamining the crystallization of poly(ε-caprolactone) and isotactic polypropylene under hard confinement: nucleation and orientation. *Macromolecules* **2017**, *50*, 9015–9023.
107 Su, C.; Shi, G.; Li, X.; Zhang, X.; Müller, A. J.; Wang, D.; Liu, G. Uniaxial and mixed orientations of poly(ethylene oxide) in nanoporous alumina studied by X-ray pole figure analysis. *Macromolecules* **2018**, *51*, 9484–9493.
108 Zhao, W.; Su, Y.; Wen, X.; Wang, D. Manipulating crystallization behavior of poly(ethylene oxide) by functionalized nanoparticle inclusion. *Polymer* **2019**, *165*, 28–38.
109 Lutkenhaus, J. L.; McEnnis, K.; Serghei, A.; Russell, T. P. Confinement effects on crystallization and curie transitions of poly(vinylidene fluoride-*co*-trifluoroethylene). *Macromolecules* **2010**, *43*, 3844–3850.
110 Maiz, J.; Martin, J.; Mijangos, C. Confinement effects on the crystallization of poly(ethylene oxide) nanotubes. *Langmuir* **2012**, *28*, 12296–12303.
111 Barrau, S.; Vanmansart, C.; Moreau, M.; Addad, A.; Stoclet, G.; Lefebvre, J. M.; Seguela, R. Crystallization behavior of carbon nanotube-polylactide nanocomposites. *Macromolecules* **2011**, *44*, 6496–6502.
112 Strawhecker, K. E.; Manias, E. Crystallization behavior of poly(ethylene oxide) in the presence of Na^+ montmorillonite fillers. *Chem. Mater.* **2003**, *15*, 844–849.
113 Szklarz, G.; Adrjanowicz, K.; Tarnacka, M.; Pionteck, J.; Paluch, M. Confinement-induced changes in the glassy dynamics and crystallization behavior of supercooled fenofibrate. *J. Phys. Chem. C* **2018**, *122*, 1384–1395.
114 Wu, D.; Cheng, Y.; Feng, S.; Yao, Z.; Zhang, M. Crystallization

https://doi.org/10.1007/s10118-020-2380-3

behavior of polylactide/graphene composites. *Ind. Eng. Chem. Res.* **2013**, *52*, 6731–6739.
115 Haggenmueller, R.; Fischer, J. E.; Winey, K. I. Single wall carbon nanotube/polyethylene nanocomposites: nucleating and templating polyethylene crystallites. *Macromolecules* **2006**, *39*, 2964–2971.
116 Steinhart, M.; Göring, P.; Dernaika, H.; Prabhukaran, M.; Gösele, U. Coherent kinetic control over crystal orientation in macroscopic ensembles of polymer nanorods and nanotubes. *Phys. Rev. Lett.* **2006**, *97*, 027801.
117 Kołodziejczyk, K.; Tarnacka, M.; Kamińska, E.; Dulski, M.; Kamiński, K.; Paluch, M. Crystallization kinetics under confinement manipulation of the crystalline form of salol by varying pore diameter. *Cryst. Growth Des.* **2016**, *16*, 1218–1227.
118 Hu, T.; Tian, N.; Ali, S.; Wang, Z.; Chang, J.; Huang, N.; Li, L. Polymer-ion interaction weakens the strain-rate dependence of extension-induced crystallization for poly(ethylene oxide). *Langmuir* **2016**, *32*, 2117–2126.
119 Su, C.; Shi, G.; Wang, D.; Liu, G. A model for the crystal orientation of polymers confined in 1D nanocylinders. *Acta Polymerica Sinica* (in Chinese) **2019**, *50*, 281–290.
120 Vanroy, B.; Wübbenhorst, M.; Napolitano, S. Crystallization of thin polymer layers confined between two adsorbing walls. *ACS Macro Lett.* **2013**, *2*, 168–172.
121 Dai, X.; Li, H.; Ren, Z.; Russell, T. P.; Yan, S.; Sun, X. Confinement effects on the crystallization of poly(3-hydroxybutyrate). *Macromolecules* **2018**, *51*, 5732–5741.
122 Zhao, W.; Su, Y.; Gao, X.; Qian, Q.; Chen, X.; Wittenbrink, R.; Wang, D. Confined crystallization behaviors in polyethylene/silica nanocomposites: synergetic effects of interfacial interactions and filler network. *J. Polym. Sci., Part B: Polym. Phys.* **2017**, *55*, 498–505.
123 Zhao, W.; Su, Y.; Gao, X.; Xu, J.; Wang, D. Interfacial effect on confined crystallization of poly(ethylene oxide)/silica composites. *J. Polym. Sci., Part B: Polym. Phys.* **2016**, *54*, 414–423.
124 Wu, L.; Lisowski, M.; Talibuddin, S.; Runt, J. Crystallization of poly(ethylene oxide) and melt-miscible PEO blends. *Macromolecules* **1999**, *32*, 1576–1581.
125 Martín, J.; Mijangos, C.; Sanz, A.; Ezquerra, T. A.; Nogales, A. Segmental dynamics of semicrystalline poly(vinylidene fluoride) nanorods. *Macromolecules* **2009**, *42*, 5395–5401.
126 Blaszczyk-Lezak, I.; Hernández, M.; Mijangos, C. One dimensional PMMA nanofibers from AAO templates evidence of confinement effects by dielectric and raman analysis. *Macromolecules* **2013**, *46*, 4995–5002.
127 Napolitano, S.; Wübbenhorst, M. Structural relaxation and dynamic fragility of freely standing polymer films. *Polymer* **2010**, *51*, 5309–5312.
128 Forrest, J. A.; Dalnoki-Veress, K.; Stevens, J. R.; Dutcher, J. R. Effect of free surfaces on the glass transition temperature of thin polymer films. *Phys. Rev. Lett.* **1996**, *77*, 2002–2005.
129 Bäumchen, O.; McGraw, J. D.; Forrest, J. A.; Dalnoki-Veress, K. Reduced glass transition temperatures in thin polymer films: surface effect or artifact? *Phys. Rev. Lett.* **2012**, *109*, 055701.
130 Sharp, J. S.; Forrest, J. A. Free surfaces cause reductions in the glass transition temperature of thin polystyrene films. *Phys. Rev. Lett.* **2003**, *91*, 235701.
131 Teichroeb, J. H.; Forrest, J. A. Direct imaging of nanoparticle embedding to probe viscoelasticity of polymer surfaces. *Phys. Rev. Lett.* **2003**, *91*, 016104.
132 Zuo, B.; Liu, Y.; Liang, Y.; Kawaguchi, D.; Tanaka, K.; Wang, X. Glass transition behavior in thin polymer films covered with a surface crystalline layer. *Macromolecules* **2017**, *50*, 2061–2068.
133 Forrest, J. A.; Dalnoki-Veress, K.; Dutcher, J. R. Interface and chain confinement effects on the glass transition temperature of thin polymer films. *Phys. Rev. E* **1997**, *56*, 5705–5716.
134 Dalnoki-Veress, K.; Forrest, J. A.; Murray, C.; Gigault, C.; Dutcher, J. R. Molecular weight dependence of reductions in the glass transition temperature of thin, freely standing polymer films. *Phys. Rev. E* **2001**, *63*, 031801.
135 Mattsson, J.; Forrest, J. A.; Börjesson, L. Quantifying glass transition behavior in ultrathin free-standing polymer films. *Phys. Rev. E* **2000**, *64*, 5187–5200.
136 Zuo, B.; Liu, Y.; Wang, L.; Zhu, Y.; Wang, Y.; Wang, X. Depth profile of the segmental dynamics at a poly(methyl methacrylate) film surface. *Soft Matter* **2013**, *9*, 9376–9384.
137 Chai, Y.; Salez, T.; McGraw, J. D.; Benzaquen, M.; Dalnoki-Veress, K.; Raphaël, E.; Forrest, J. A. A direct quantitative measure of surface mobility in a glassy polymer. *Science* **2014**, *343*, 994–999.
138 Fakhraai, Z.; Forrest, J. A. Measuring the surface dynamics of glassy polymers. *Science* **2008**, *319*, 600–604.
139 Page, K. A.; Kusoglu, A.; Stafford, C. M.; Kim, S.; Kline, R. J.; Weber, A. Z. Confinement-driven increase in ionomer thin-film modulus. *Nano Lett.* **2014**, *14*, 2299–2304.
140 Lee, J. H.; Chung, J. Y.; Stafford, C. M. Effect of confinement on stiffness and fracture of thin amorphous polymer films. *ACS Macro Lett.* **2012**, *1*, 122–126.
141 Torres, J. M.; Stafford, C. M.; Vogt, B. D. Elastic modulus of amorphous polymer thin films: relationship to the glass transition temperature. *ACS Nano* **2009**, *3*, 2677–2685.
142 Torres, J. M.; Wang, C.; Coughlin, E. B.; Bishop, J. P.; Register, R. A.; Riggleman, R. A.; Stafford, C. M.; Vogt, B. D. Influence of chain stiffness on thermal and mechanical properties of polymer thin films. *Macromolecules* **2011**, *44*, 9040–9045.
143 Liu, Y.; Chen, Y. C.; Hutchens, S.; Lawrence, J.; Emrick, T.; Crosby, A. J. Directly measuring the complete stress-strain response of ultrathin polymer films. *Macromolecules* **2015**, *48*, 6534–6540.
144 Chang, J.; Toga, K. B.; Paulsen, J. D.; Menon, N.; Russell, T. P. Thickness dependence of the Young's modulus of polymer thin films. *Macromolecules* **2018**, *51*, 6764–6770.
145 Tweedie, C. A.; Constantinides, G.; Lehman, K. E.; Brill, D. J.; Blackman, G. S.; Vliet, K. J. V. Enhanced stiffness of amorphous polymer surfaces under confinement of localized contact loads. *Adv. Mater.* **2007**, *19*, 2540–2546.
146 Yoon, H.; McKenna, G. B. "Rubbery stiffening" and rupture behavior of freely standing nanometric thin PIB films. *Macromolecules* **2017**, *50*, 9821–9830.
147 Bay, R. K.; Shimomura, S.; Liu, Y.; Ilton, M.; Crosby, A. J. Confinement effect on strain localizations in glassy polymer films. *Macromolecules* **2018**, *51*, 3647–3653.
148 Boissé, S. P.; Kryuchkov, M. A.; Tien, N. D.; Bazuin, C. G. R.; Prud'homme, R. E. PLLA crystallization in linear AB and BAB copolymers of L-lactide and 2-dimethylaminoethyl methacrylate. *Macromolecules* **2016**, *49*, 6973–6986.
149 Boschetti-de-Fierro, A.; Lorenzo, A. T.; Müller, A. J.; Schmalz, H.; Abetz, V. Crystallization kinetics of PEO and PE in different triblock terpolymers: effect of microdomain geometry and confinement. *Macromol. Chem. Phys.* **2008**, *209*, 476–487.
150 Gan, Z.; Jiang, B.; Zhang, J. Poly(ε-caprolactone)/poly(ethylene oxide) diblock copolymer 1. Isothermal crystallization and melting behavior. *J. Appl. Polym. Sci.* **1996**, *59*, 961–967.
151 Chen, H. L.; Hsiao, S. C.; Lin, T. L.; Yamauchi, K.; Hasegawa, H.; Hashimoto, T. Microdomain-tailored crystallization kinetics of block copolymers. *Macromolecules* **2001**, *34*, 671–674.
152 Chen, H. L.; Wu, J. C.; Lin, T. L.; Lin, J. S. Crystallization kinetics in microphase-separated poly(ethylene oxide)-block-poly(1,4-butadiene). *Macromolecules* **2001**, *34*, 6936–6944.
153 Hillmyer, M. A.; Bates, F. S. Influence of crystallinity on the morphology of poly(ethylene oxide) containing diblock

https://doi.org/10.1007/s10118-020-2380-3

copolymers. *Macromol. Symp.* **1997**, *117*, 121–130.
154 Ho, R. M.; Lin, F. H.; Tsai, C. C.; Lin, C. C.; Ko, B. T.; Hsiao, B. S.; Sics, I. Crystallization-induced undulated morphology in polystyrene-*b*-poly(L-lactide) block copolymer. *Macromolecules* **2004**, *37*, 5985–5994.
155 Kofinas, P.; Cohen, R. E. Morphology of highly textured poly(ethylene)/poly(ethylene-propylene) (E/EP) semicrystalline diblock copolymers. *Macromolecules* **1994**, *27*, 3002–3008.
156 Loo, Y. L.; Register, R. A.; Ryan, A. J. Modes of crystallization in block copolymer microdomains: breakout, templated, and confined. *Macromolecules* **2002**, *35*, 2365–2374.
157 Loo, Y.-L.; Register, R. A.; Ryan, A. J.; Dee, G. T. Polymer crystallization confined in one, two, or three dimensions. *Macromolecules* **2001**, *34*, 8968–8977.
158 Mai, S. M.; Fairclough, J. P. A.; Viras, K.; Gorry, P. A.; Hamley, I. W.; Ryan, A. J.; Booth, C. Chain folding in semicrystalline oxyethylene/oxybutylene diblock copolymers. *Macromolecules* **1997**, *30*, 8392–8400.
159 Quiram, D. J.; Register, R. A.; Marchand, G. R. Crystallization of asymmetric diblock copolymers from microphase-separated melts. *Macromolecules* **1997**, *30*, 4551–4558.
160 Xu, J. T.; Fairclough, J. P. A.; Mai, S. M.; Ryan, A. J.; Chaibundit, C. Isothermal crystallization kinetics and melting behavior of poly(oxyethylene)-*b*-poly(oxybutylene)/poly(oxybutylene) blends. *Macromolecules* **2002**, *35*, 6937–6945.
161 Xu, J. T.; Turner, S. C.; Fairclough, J. P. A.; Mai, S. M.; Ryan, A. J.; Chaibundit, C.; Booth, C. Morphological confinement on crystallization in blends of poly(oxyethylene-block-oxybutylene) and poly(oxybutylene). *Macromolecules* **2002**, *35*, 3614–3621.
162 Zuo, B.; Xu, J.; Sun, S.; Liu, Y.; Yang, J.; Zhang, L. Stepwise crystallization and the layered distribution in crystallization kinetics of ultra-thin poly(ethylene terephthalate) film. *J. Chem. Phys.* **2016**, *144*, 234902.
163 DeFelice, J.; Milner, S. T.; Lipson, J. E. G. Simulating local T_g reporting layers in glassy thin films. *Macromolecules* **2016**, *49*, 1822–1833.
164 Tito, N. B.; Lipson, J. E. G.; Milner, S. T. Lattice model of dynamic heterogeneity and kinetic arrest in glass-forming liquids. *Soft Matter* **2013**, *9*, 3173–3180.
165 Lang, R. J.; Merling, W. L.; Simmons, D. S. Combined dependence of nanoconfined T_g on interfacial energy and softness of confinement. *ACS Macro Lett.* **2014**, *3*, 758–762.
166 Hsiao, M.-S.; Chen, W. Y.; Zheng, J. X.; Horn, R. M. V.; Quirk, R. P.; Ivanov, D. A.; Thomas, E. L.; Lotz, B.; Cheng, S. Z. D. Poly(ethylene oxide) crystallization within a one-dimensional defect-free confinement on the nanoscale. *Macromolecules* **2008**, *41*, 4794–4801.
167 Zhu, L.; Cheng, S. Z. D.; Calhoun, B. H.; Ge, Q.; Quirk, R. P.; Thomas, E. L.; Hsiao, B. S.; Yeh, F.; Lotz, B. Crystallization temperature-dependent crystal orientations within nanoscale confined lamellae of a self-assembled crystalline-amorphous diblock copolymer. *J. Am. Chem. Soc.* **2000**, *122*, 5957–5967.
168 Zhu, L.; Cheng, S. Z. D.; Calhoun, B. H.; Ge, Q.; Quirk, R. P.; Thomas, E. L.; Hsiao, B. S.; Yeh, F.; Lotz, B. Phase structures and morphologies determined by self-organization, vitrification, and crystallization: confined crystallization in an ordered lamellar phase of PEO-*b*-PS diblock copolymer. *Polymer* **2001**, *42*, 5829–5839.
169 Floudas, G.; Tsitsilianis, C. Crystallization kinetics of poly(ethylene oxide) in poly(ethylene oxide)-polystyrene-poly(ethylene oxide) triblock copolymers. *Macromolecules* **1997**, *30*, 4381–4390.
170 Ho, R. M.; Chiang, Y. W.; Lin, C. C.; Huang, B. H. Crystallization and melting behavior of poly(*ε*-caprolactone) under physical confinement. *Macromolecules* **2005**, *38*, 4769–4779.
171 Wang, H.; Keum, J. K.; Hiltner, A.; Baer, E. Crystallization kinetics of poly(ethylene oxide) in confined nanolayers. *Macromolecules* **2010**, *43*, 3359–3364.

https://doi.org/10.1007/s10118-020-2380-3